Towards an End-to-End Analysis and Prediction System for Weather, Climate, and Marine Applications in the Red Sea

Ibrahim Hoteit, Yasser Abualnaja, Shehzad Afsal, Boujemaa Ait El Fquih, Triantaphyllos Akylas, Charls Antony, Clint Dawson, Khaled Asfahani, Robert J W Brewin, Luigi Cavaleri, et al.

Integrated Data-Driven Modeling Solutions / Services ??? for Weather, Climate, and Marine Applications in the Red Sea

Or???

Towards a Seamless Prediction System for Weather, Climate, and Marine Applications in the Red Sea

Ibrahim Hoteit[1,1], Yasser Abualnaja[1], Shehzad Afsal[1], Boujemaa Ait-El-Fquih[1], Triantaphyllos Akylas[2], Samah El-Mohtar[1], Charls Antony[1], Clint Dawson[3], Khaled Asfahani[4], Robert Brewin[5], Luigi Cavaleri[6], Ivana Cerovecki[7], Bruce Cornuelle[7], Srinivas Desamsetti[8], Raju Attada[1], Hari Dasari[1], Jose Sanchez-Garrido[9], Lily Genevier[1], Mohamad Gharamti[10], John Gittings[1], Elamurugu Gokul[1], Ganesh Gopalakrishnan[7], Daquan Guo[1], Bilel Hadri[1], Markus Hadwiger[1], Mohammed Abed Hammoud[1], Myrl Hendershott[7], Mohamad Hittawe[1], Ashok Karumuri[11], Armin Köhl[12], Samuel Kortas[1], Omar Knio[1], George Krokos[1], Ravi Kunchala[13], Sabique Langodan[1], Thong Luong[1], Olivier Le-Maitre[14], Pierre Lermusiaux[2], Jingyi Ma[1], Vassilis Papadopoulos[15], Trevor Platt[16], Larry Pratt[17], Naila Raboudi[1], Marie-Fanny Racault[16], Shanas Razak[1], Dionysios Raitsos[18], Shuba Sathyendranath[16], Sanikommu SivaReddy[1], Sarantis Sofianos[18], Aneesh Subramanian[19], Rui Sun[7], Edriss Titi[20], Habib Toye[1], George Triantafyllou[15], Kostas Tsiaras[15], Panagiotis Vasou[1], Yesubabu Viswanadhapalli[21], Yixin Wang[1], Fengchao Yao[1], Peng Zhan[1]

[1] Physical Sciences and Engineering Division, King Abdullah University of Science and Technology (KAUST), Thuwal, Saudi Arabia

[2] Massachusetts Institute of Technology (MIT), Cambridge, Massachusetts, USA

[3] The University of Texas at Austin, Austin, Texas, USA

[4] Saudi Aramco, Damam, Saudi Arabia

[5] University of Exeter, Cornwall, United Kingdom

[6] Institute of Marine Sciences, Venice, Italy

[7] Scripps Institution of Oceanography, La Jolla, California, USA

[8] National Center for Medium Range Weather Forecasting (NCMRWF), Noida, India

[9] University of Malaga, Spain

[10] National Center of Atmospheric Research (NCAR), Boulder, Colorado, USA

[11] University of Hyderabad, Hyderabad, India

[12] University of Hamburg, Hamburg, Germany

[13] Indian Institute of Technology, Delhi, India

[14] Ecole Polytechnique, Palaiseau, France

[15] Hellenic Centre for Marine Research (HCMR), Anavissos, Greece

[16] Plymouth Marine Laboratory (PML), Plymouth, United Kingdom

[1] *Corresponding author*: ibrahim.hoteit@kaust.edu.sa

[17] Woods Hole Oceanographic Institution (WHOI), Woods Hole, Massachusetts, USA
[18] National and Kapodistrian University of Athens, Athens, Greece
[19] University of Colorado, Boulder, Colorado, USA
[20] University of Cambridge, Cambridge, United Kingdom
[21] National Atmospheric Research Laboratories (NARL), Gadanki, India

Abstract

The Red Sea (RS), home to the second-largest coral reef system, is a vital resource for the Kingdom of Saudi Arabia. Tourism, agriculture and fishing industries together contribute about 10-20% of the country's GDP, and 90% of the Kingdom's potable water is desalinated from the sea. All these activities, and those elsewhere in the RS region, critically depend on vagaries of oceanic and atmospheric conditions.

In the background of mega-developments projects along the RS coast, depleting petro-resources, and global warming, authorities are working on optimized harnessing of environmental resources, including renewable energy, rainwater harvesting, etc. These require high-resolution weather and climate information. Toward this end, we have adopted a multi-pronged R&D activity in which we developed an integrated data-driven regional coupled modeling system. The telescopic components include 5km-600m resolution regional-atmospheric models to address weather and climate challenges, 4km-50m resolution ocean models with regional and coastal configurations to simulate/predict the general circulation and mesoscale dynamics, a 4km-100m ecosystem model to simulate the biogeochemistry, and 1km-50m resolution wave models. In addition, a complementary probabilistic transport modeling system predicts dispersion of contaminant plumes, oil-spill, and marine ecosystem connectivity. Advanced ensemble data assimilation capabilities have been also implemented for accurate forecasting.

Resultant achievements include unprecedented understanding of the regional circulation and its connection to the global climate, generation and validation of long-term RS regional atmospheric-oceanic-wave reanalyses, and forecasting capacities. These are being extensively used by researchers/government/industry in various weather and marine studies and operations, environmental policies, renewable energy applications, impact assessment, flood-forecasting, etc.

1. **Introduction**

The Red Sea is a semi-enclosed, elongated marginal sea of the Indian Ocean, lying between Africa and Asia. This Large Marine Ecosystem (LME) is connected to the Indian Ocean through the Strait of Bab-al-Mandeb (BaM) and to the Mediterranean through the Suez Canal (Fig.1). As a vital resource of fisheries, agriculture, tourism, freshwater through desalination, and a major shipping route, the Red Sea is of paramount political and economic importance both for the region and the world. Influenced by distinct geological, atmospheric, and hydrographic settings, the Red Sea is a unique LME characterized by the second longest and world third largest coral reef system thriving under one of the warmest and most saline conditions of the world oceans (Edwards and Head 1986). The Red Sea presents all major oceanographic processes, but at much smaller spatiotemporal scales compared to the global ocean, making it an ideal test basin for studies on ocean-climate interactions, as it is expected to exhibit a faster response to the global climate variations (Belkin 2009; Carvalho et al. 2019). Despite its political, economic and scientific importance, the Red Sea remains a vastly under-explored region.

With an average width of 280 km, length of 2000 km, and maximum depths of above 2500 m along the axial trench, the Red Sea is a geologically young ocean. Nested between 12.5 ºN to 30 ºN in the NW-SE direction, it has a constricted connection with the Gulf of Aden, with a maximum depth of only 137 m at the Hanish Sill. The bathymetry varies from extensive shallow shelves with depths < 50 m in the south to steep-sloped basins with depths > 800 m in the north.

The atmospheric conditions over the Red Sea are mainly influenced by the arid surrounding terrestrial environment, the seasonal Indian monsoon system and the orographic effects of the coastal mountains, with the resultant atmospheric forcing exhibiting marked variability on various time scales (Viswanadhapalli et al. 2017). As a result of the arid climate, the annual mean net freshwater loss due to excessive evaporation over precipitation is estimated to ~2 m yr^{-1}, and the heat flux has a relatively small annual mean heat loss of 11 W m^{-2}, but a large annual cycle with a range of ~200 W m^{-2}. Channeled by the coastal mountains, the surface winds tend to flow along the direction of the axis of the Red Sea. In summer (June to September) they generally blow northwesterly throughout the whole basin, whereas in winter they reverse from southeasterly to northwesterly in the southern Red Sea, creating a convergence zone around 18 °N (Langodan et al. 2014). On smaller spatial scales, intense across-basin winds flowing between the coastal mountain gaps are also observed, the most prominent of which is the Tokar jet at around 18 °N of the African coast. North of 20 °N, the mountain-gap winds usually originate from the Arabian subcontinent and gush westward.

In response to the atmospheric forcing and limited exchanges with the Indian Ocean, the Red Sea acts as a concentration basin, producing one of the world saltiest water masses through complex two-layer overturning system (Fig.2). On an annual mean basis, an overturning cell lies in the upper layer around the sill depth in the south and deepens to about 300 m in the north. It is composed of a northward surface inflow from the Gulf of Aden and an intermediate southward flow (Sofianos and Johns 2007). This layer is directly subject to the annual cycle of surface heat flux and freshwater loss, resulting in marked

seasonal surface temperature variations and a northward increase in surface salinity (Sofianos and Johns 2015). The Red Sea intermediate water is formed in the north during winter and is exported into the Gulf of Aden through BaM, driving a two-layer water exchange structure (Sofianos and Johns 2007). During summer, the above overturning circulation and water exchange structure in the strait reverse, following the onset of the Indian summer monsoon (Yao et al. 2014a,b). An intermediate water intrusion at depths 50 – 100 m is induced from the Gulf of Aden, the mean surface currents change to flow southward, and the water exchange in BaM switches to a three-layer structure with the deep outflow significantly suppressed. The lower layer of the overturning system, extending to the basin bottom, is occupied by a nearly homogeneous warm (~21.5°C) and highly saline (~40.5) water mass, which is usually referred to as the Red Sea Deep Water (RSDW). Nevertheless, a deep circulation with a southward bottom flow and an intermediate northward returning flow centered around a depth of 500 m is suggested by geochemical tracers and dissolved oxygen gradients (Cember 1988; Eshel et al. 1994).

Despite being characterized as an oligotrophic large marine ecosystem, the Red Sea is a region of remarkable biodiversity and endemism and hosts one of the world's largest coral reef ecosystems (Carvalho et al. 2019). The functioning of the Red Sea ecosystem is highly governed by the environmental conditions, which modulate it on different levels (Triantafyllou et al. 2014). The Red Sea has been subject to warming trends (Raitsos et al. 2011; Chaidez et al. 2017; Krokos et al. 2019a) which led to coral reef bleaching events (Cantin et al. 2010; Osman et al. 2018; Genevier et al. 2019) and significant impacts on its productivity (Raitsos et al. 2015, Gittings et al. 2018). The Red Sea ecosystem, with its relatively simple-shaped and semi-enclosed basin, high biodiversity and rich dynamics, provides the scientific community with an accessible, ideal natural laboratory to study the physical-biological interactions on different spatial and temporal scales.

Until recently, the Red Sea region remained generally underdeveloped. The last decade has, however, witnessed an unprecedented increase in population and an acceleration in residential, commercial and industrial developments along the Red Sea coast. NEOM, short for the Latin-Arabic term Neo-Mustaqbal, signifying "new future", is a $500bn mega-project that aims to build a fully-automated city operating as an independent economic zone in the northwestern part of Saudi Arabia. The Red Sea Project is another mega-development along the central Saudi coast and is intended to transform the Red Sea coast into a world-class tourist destination, whose blueprint is primarily based on a coastal lagoon with 90-plus pristine islands.

Maintaining a sustainable, healthy marine environment is a core objective of these developments. In this context, understanding and forecasting the regional weather through climate variations is essential for a wide variety of high-impact societal needs, including environmental protection and coastal management, weather extremes, pollution and contamination, exploration and drilling, accidents response, desalination and plant cooling operations, shipping, harbor management and national security operations, management of fisheries and marine aquaculture, water resources, renewable energy, etc. Given the unique structure of the Red Sea basin and surrounding deserts, and the ocean and atmospheric

connections to the global circulation, the need for integrated state-of-the-art modeling and supporting datasets is acute.

The newly established King Abdullah University of Science and Technology (KAUST) acts as a hub of frontline research in the biological, physical, geological aspects of the Red Sea region. In this context, KAUST dedicated important resources for studying the Red Sea and understanding its resources, with the goal of preserving its fragile ecosystem while at the same time supporting the local authorities to exploit its unique resources. In parallel to the on-going hydrographic and ecological observational efforts, and through sustained and strong collaborations with many international organizations, the Red Sea Modelling and Prediction group at KAUST has led the development of a comprehensive and integrated modeling and prediction system to study, monitor and predict the atmospheric and oceanic phenomena of the region. The system is being built by fully integrating atmospheric and oceanic circulations, surface wave, air pollution, dust, marine biogeochemistry, and advanced data analytics and visualization, achieving remarkable progress in the short span of a decade. The modeling system also relies on *in situ* and remotely-sensed observations (detailed in the supplementary materials) for the purpose of validation and data assimilation and provides insights into the systematic relations between the interactions of different components and the management of various applications.

An important achievement from this effort is the first high-resolution atmospheric reanalyses for the region from 1980 till present, generated using our assimilative atmospheric modeling system, which is turning out to be critical not only for the Red Sea climate research, but also contributing to Indian monsoon studies. This regional reanalysis is being used to force the MIT ocean general circulation model (MITgcm), the WaveWatch-III (WWIII) model, and various transport models that have been tuned to the Red Sea environment. Notably, these capabilities are currently being extensively used to support various industrial and governmental developments. In this paper, we elaborate on our state-of-the-art modeling and forecasting technologies, their applications, our achievements in science and contributions to the industry. Section 2 provides a detailed description of our integrated data-driven Red Sea Modeling system version 1 (iReds-M1). We catalogue some of our salient science findings and industrial applications in Section 3. We briefly present our future plans in the concluding Section.

2. **The integrated Red Sea Model (iReds-M1)**

iReds-M1 is a sophisticated and comprehensive system, which enables the community to make a great leap in the climate variability research on the understudied Red Sea region. It comprises a set of state-of-the-art modeling components for simulating the atmosphere, ocean, waves, transports, and bio-geochemistry (as schematized in Fig.3). A description of the components follows.

The atmospheric models: The Advanced Weather Research and Forecasting (WRF) model (Skamarock et al. 2008), developed by the US National Centers for Environmental Prediction (NCEP), is a state-of-the-art mesoscale model offering numerous advanced physics options for simulating atmospheric

processes at various scales, and also provides a robust and flexible platform for assimilation. In various baseline studies, we used the model to simulate the mean regional climate of the Arabian Peninsula (AP) and its interannual variability (Viswanadhapalli et al. 2017; Langodan et al. 2017a; Dasari et al. 2017b; Attada et al. 2018a,b,c). The model was successful in delineating the structure and climatology of the monsoon low-level jet and monsoon inversion over the Arabian Sea (Viswanadhapalli et al. 2019). We also used it to carry out detailed assessments of renewable energy resources in the AP (Langodan et al. 2016a; Dasari et al. 2019a), and for predicting extreme heavy rainfall events (Viswanadhapalli et al. 2016; Dasari et al. 2017b; Luong et al. 2019).

We have implemented WRF in assimilation mode at 5-km resolution with the ECMWF global reanalysis as initial and boundary conditions to develop the first high-resolution regional reanalysis for the region from 1980 till present (Viswanadhapalli et al. 2017; Langodan et al., 2017a,b). Available satellite and conventional observations in the AP were assimilated. The reanalysis fields are extensively being used to study, for instance, the regional met-ocean conditions (e.g., Viswanadhapalli et al. 2017, 2019), to provide vital information about the background state of the regional environment (e.g., Dasari et al. 2019c), and to force our ocean models (e.g., Langodan et al. 2014, 2016a; Zhan et al. 2019; Krokos et al. 2019b).

In addition, to simulate air parcel trajectories as well as transport, dispersion, chemical transformation, and deposition, we use the Hybrid Single-Particle Lagrangian Integrated Trajectory (HYSPLIT) (Draxler et al. 1997). The model, forced with specially-generated WRF forcing at 600 m resolution, was recently used to investigate the distributions of air pollutants concentration at various sites along the Red Sea coast, including the NEOM and RSP regions (Dasari et al. 2019c).

The ocean components: The Red Sea circulation is simulated using a 1-km resolution MITgcm (Marshall et al. 1997a,b). The model domain covers the entire Red Sea including the two gulfs (Suez and Aqaba) at the north end, with an open boundary in the Gulf of Aden. The model topography is generated based on the General Bathymetric Chart of the Ocean (Ioc, 2003), updated with available regional data. The eastern open boundary conditions are extracted on a daily basis from the latest ocean reanalysis product GLORYS2 by Mercator Ocean (http://marine.copernicus.eu/). To resolve the different frequencies of water elevation variations (Churchill et al. 2018), the normal velocity at the boundary is adjusted to match the volume flux of GLORYS2. The model is forced with hourly fields from our high-resolution WRF downscaled fields, including surface wind, air temperature, specific humidity, precipitation, and downward short-wave and long-wave radiation. The Red Sea MITgcm outputs were validated against different datasets and in various settings and applications. These include studying the general and overturning circulation (Yao et al. 2014a,b), the mixed layer variations (Krokos et al. 2019b), the deep water formation events (Yao and Hoteit 2018), the eddies characteristics (Zhan et al. 2014; 2016; 2019), the Red Sea internal/baroclinic tides (Guo et al. 2018), phytoplankton phenology (bloom timing) in the southern (Dreano et al. 2016) and northern Red Sea (Gittings et al. 2018). The adjoint model of MITgcm

is being further used to conduct sensitivity studies of quantities-of-interest with respect to the model states and atmospheric forcings across the Red Sea (Zhan et al. 2018).

WWIII (Tolman 2008), the third-generation wave model developed at the NOAA/NCEP, is used to simulate the waves in the Red Sea at 1-km resolution. The model is configured with 33 frequencies, starting from 0.05 Hz and 36 equally spaced directions and the most recent physics formulation (Ardhuin et al. 2010). The validated model outputs (Langodan et al. 2014) were analysed to assess the impact of atmospheric data assimilation on waves predictions (Langodan et al. 2016b), to investigate the physical aspects of the unique seasonally opposing wind-wave systems in the central Red Sea (Langodan et al. 2015), to quantify the wave energy potentials (Langodan et al. 2016a), and to study the wind-wave climate and it's trends (Langodan et al. 2017a,b; 2018; 2019b).

Transport phenomena are simulated using the Connectivity Modelling System (CMS), a multi-scale probabilistic model of particle dispersal (Paris et al. 2013). CMS driven by the MITgcm flow fields has been successfully implemented to study concentrate discharges (Zhan et al. 2015), biological connectivity among different coral reef complexes at coastal (Nanninga et al. 2015), basin (Raitsos et al. 2017), and cross-basin scales (Wang et al. 2019). Oil spill transport and weathering processes are simulated with MEDSLIK (De Dominicis et al. 2013a,b) as Lagrangian particles transported by ocean currents, wind and waves, and a stochastic displacement that parameterizes turbulent diffusion.

The biogeochemical cycle is simulated using the European Regional Seas Ecosystem Model (ERSEM) (Baretta et al. 1995). ERSEM is a generic comprehensive model that has been successfully implemented across a wide range of coastal and open ocean ecosystems (e.g., Petihakis et al. 2002; Collingridge 2012). The model is based on a 'functional' group approach, using size as the major biotic group characteristic. The pelagic model food web consists of four phytoplankton groups, bacteria and three zooplankton groups, and is coupled with the associated benthic model that includes the settling of organic detritus into the benthos and diffusional nutrient fluxes out of the sediment. The pelagic variables include particulate and dissolved organic matter, along with dissolved inorganic nutrients, allowing the coupling of biologically driven carbon dynamics with the chemical dynamics. ERSEM forced with the outputs of our MITgcm and WRF models has been implemented by Triantafyllou et al. (2014), successfully reproducing the main seasonal features of the Red Sea ecosystem.

Coastal ocean modeling: To simulate the complex coastal processes, we implemented ocean models specifically designed for coastal and engineering applications. These include (i) the Delft3d model (Deltares 2016) to simulate the coastal circulations, including flow induced by tides, wind, and sediment transport, (ii) the shallow-water Advanced CIRCulation (ADCIRC) model (Luettich and Westerink 2004) to simulate water level variations and surges on an unstructured grid that enables to resolve in details near-shorelines at extreme resolutions, and (iii) the Simulating Waves Nearshore (SWAN) model (Booji et al. 1999) that is coupled with both Delft3D and ADCIRC and designed for simulating short crested waves in coastal environments.

The coupled WRF-MITgcm-WWIII system: Ocean temperatures over the Red Sea region play an important role in modulating the region's weather and climate (Gimeno et al. 2010; Sun et al. 2019). Furthermore, while most of the AP experiences hot and dry summers, the conditions in coastal regions east of the Red Sea are relatively cooler and humid owing to transported moisture from the Red Sea. The Scrips-KAUST Regional Integrated Prediction System (SKRIPS) is a new regional coupled ocean-atmosphere WRF+MITgcm+WWIII system that was developed to study air-sea feedbacks in the Red Sea region and to build long-term regional forecasting capabilities (Sun et al. 2019). The coupling between these components is implemented based on the Earth System Modeling Framework (ESMF) (Hill et al. 2004) and the interfaces are implemented according to the National United Operational Prediction Capability (NUOPC) consortium. This regional coupled model allows for the oceanic mixed layer heat and momentum to interact with the atmospheric boundary layer dynamics at the mesoscale and higher resolution. This should reproduce feedbacks that cannot be well-resolved by coarse-resolution global coupled models and are absent in regional uncoupled models. SKRIPS was implemented to investigate the heatwaves in the Red Sea region on seasonal scales, demonstrating that the evolving ocean temperatures considerably improves the prediction of the amplitude of these heatwaves, particularly in the coastal region (Sun et al. 2019).

Data assimilation: Assimilation is a process by which a model is constrained towards available observations to obtain improved forecasts/hindcasts. Our atmospheric and ocean general circulation models are equipped with state-of-the-art assimilation packages; the Data Assimilation Research Testbed – DART (Hoteit et al., 2014), which comprises advanced ensemble schemes (Anderson et al. 2009) and the adjoint-based ECCO inverse system (Stammer et al. 2002) for MITgcm, and the extensive assimilation package of WRF (Barker, 2012), which also includes DART. We are currently employing a cyclic 3DVAR for assimilation with WRF (3DVAR-WRF; Viswanadhapalli et al. 2017) and an ensemble adjustment Kalman filter (EAKF) for MITgcm (Toye et al. 2017, 2018). We have recently further developed the DART-MITgcm system to operate with hybrid ensembles composed of flow-dependent and seasonally-varying static members (Toye et al. 2019), and demonstrated significant improvements when driving the MITgcm with ensembles of forcing and physics (Sivareddy et al. 2019). We are currently working on tuning DART for WRF, and of testing newly introduced ensemble assimilation schemes (Hoteit et al. 2015; Raboudi et al. 2018). The system is being further equipped with new efficient techniques for simulating transport phenomena (El-Mohtar et al. 2018) and control of unmanned vehicles (Wang et al. 2017; Albarakati et al. 2019) under the uncertainties described by the ensembles.

We assimilate a variety of observations from different networks, including satellite (e.g. Altimeter SSH and AVHRR SST in the ocean, and QuikSCAT and Advanced Scatterometer winds in the atmosphere) and land-based (e.g., weather Radars) remote sensing, station-based (e.g. oceanic temperature and salinity observations from moored buoys and ship transects, meteorological observations from synoptic stations and Metar) and freely drifting (e.g., Argo observations in the ocean, and upper-air

soundings of Rawinsonde and pilot balloon) *in situ* observations. Fig.4 is a demonstration of the significant improvement achieved after assimilation in the Red Sea.

Visualization and data analytics: Advanced visualization is an integral component of our system to support data analysis tasks for scientists and non-expert users. We have developed a visual analytics application, called RedSeaAtlas (Afzal et al. 2019a), considering the tasks, computational and operational requirements of the variety of simulation models and observational datasets of the Red Sea region. The application provides a suite of interactive visualization tools that can facilitate diverse research tasks through interactive visual exploration and analysis of spatio-temporal multivariate data (Fig.5). These include interactive feature selection, spatial and temporal filtering, overview and details-on-demand, and capability to analyze data from disparate data sources (Afzal et al. 2019b).

We have also developed an interactive visual analysis framework, called Ovis (Höllt et al. 2013, 2014), for interactive exploration and analysis of ensemble data. The core components of this framework are built based on an efficient GPU-based computation and visualization pipeline. We presented two case studies to showcase the effectiveness of this framework; the first investigated the placement planning and operation of off-shore structures related to oil and gas industry, and the second demonstrated the effectiveness of this system to plan pathways of autonomous sea vehicles (gliders) through interactive exploration and analysis of ensemble data (Höllt et al. 2013, 2015).

3. iReds Salient Contributions to Science and industry

Study of the Red Sea Region Circulation, Climate and Ecosystem

Atmospheric variability: Motivated by the background knowledge from the analysis of global fields, and to meet the need for high-resolution datasets to resolve mesoscale characteristics, we developed a regional reanalysis at 5 km resolution for a 39-year period (1980-2018). The reanalysis fields accurately reproduced the known Red Sea climatic features such as Red Sea Trough, Red Sea Convergence Zone, Arabian anti-cyclone, and seasonal circulation patterns (Viswanadhapalli et al. 2017). It has been further extensively used to drive iReds ocean models and for subsequent regional applications, and to support the mega-projects being developed along the Red Sea coast. Several studies were also conducted using convective-permitting WRF configurations to investigate the predictability of extreme rainfall and winds, presented in more detail below.

Based on global reanalyses, our study of the regional surface air temperature (SAT) suggested that it is strongly modulated by the circulation patterns (Attada et al. 2018a), and an impact of the Indian summer monsoon through westward propagating Rossby-waves (Attada et al. 2018b). Dasari et al. (2017a, 2019b) showed that the baroclinic instability induced by the intensification and southward shift of subtropical westerly jet over the AP facilitates an increase in the passage of synoptic-transients and winter

rainfall. Kunchala et al. (2018; 2019) showed a significant increasing trend in the recent decade in the summer aerosol optical depth (AOD) over AP, related to an intensification of the Tokar jet.

Ocean general circulation: The Red Sea MITgcm has provided an unprecedented description of the 3D basin circulation, and successfully simulated the upper overturning cell and its seasonal variability (Yao et al. 2014a,b; Krokos et al. 2019b). Based on long-term ocean historical simulations, Yao and Hoteit (2018) revealed the episodic nature of deep-water renewal related to specific atmospheric events and provided updated estimates of the deep-water renewal time. The model simulations together with all available hydrographic observations were also analyzed to provide a full description of the seasonal and spatial variability of the Red Sea mixed layers (MLs), revealing the roles of individual physical processes (Krokos et al. 2019b). The local Buoyancy forcing and Indian Ocean monsoon drive the overturning circulation, and ultimately modulate the water exchanges with the Gulf of Aden through BaM (Yao et al. 2014a,b). Analysis of the interannual variability of the exchanges further revealed a strong dependence on the intensity and duration of the Indian Ocean monsoon (Raitsos et al. 2013; Dreano et al. 2016; Xie et al. 2019).

The ocean and ecosystem model simulations, combined with various remote sensing datasets, have provided new insights on how ocean circulations and biogeochemical processes drive the ecosystem in the Red Sea. This unified framework led to new understandings of the interplay between physical drivers such as buoyancy fluxes and ocean mixing, and important tracers for the ecosystem functioning. Despite a limited supply of nutrients, subsurface intrusion from the Gulf of Aden and the winter deep convection drive elevated values of primary productivity in the south during summer (Raitsos et al. 2013; Dreano et al. 2016) and in the north during winter (Gittings et al. 2018). Moreover, marine larvae/planulae disperse nearly passively with the circulation, forming genetic connectivity across geographically separated reef sites within the basin (Raitsos et al. 2017), as well as between the southern Red Sea and the Indian Ocean (Wang et al. 2019).

Mesoscale circulation: The upper-layer Red Sea circulation is characterized by complex and highly varying mesoscale activities, consisting of energetic semi-permanent and transient eddies and swirling currents, with stronger activity during winter (Zhan et al. 2014). Spatially, the central and northern regions show the annual eddy kinetic energy (EKE) peaks during both seasons, whose effect on the water column may reach down to 300 m and intensifies towards the surface. The MITgcm outputs suggested that the northward gradient of heat loss tilts the density isopycnals, which gradually deepen towards the north, thereby evoking baroclinic instabilities and hence the eddies generation (Zhan et al. 2016). The EKE dominates the mean flow kinetic energy (Zhan et al. 2016), with the fate of observed eddies being largely governed by atmospheric forcing and local remote ocean conditions (Zhan et al. 2018). Driven by considerable heat fluxes, intensified eddy activity has also been shown to promote convection processes, especially during winter in the north (Papadopoulos et al. 2013). The northward transport of warmer and fresher water by eddies reduces the intrinsic meridional gradient and flattens the isopycnals, which in turn

limits the eddy generation and was interpreted as a typical negative feedback mechanism (Zhan et al. 2019). The Red Sea mesoscale circulation plays a significant role in transporting biogeochemical tracers within the basin, and have been shown to strongly impact the sensitive marine ecosystem (Zhan et al. 2014; Dreano et al. 2016; Raitsos et al. 2017).

Tides: The main tidal signal in the Red Sea propagates from the open ocean through BaM. Observations and simulations suggest a high variability of tidal elevation with latitude, with the northern and southern basins exhibiting relatively large amplitudes compared to the central basin (Guo et al. 2016). Tidal waves may also generate solitary waves, mainly at steep sides of the deep trough in the southern part of the Red Sea (da Silva et al. 2012; Guo et al. 2016). Based on our experiments with a high-resolution non-hydrostatic MITgcm, we found that the breaking of internal waves induces vertical mixing and may increase the supply of nutrients to the euphotic zone, which may enhance biological productivity by disrupting the pycnocline and inducing turbulence (Guo et al. 2019).

Waves: The wave variability in the Red Sea is naturally associated with the dominant regional wind regimes (Langodan et al. 2014). Although wind intensity in the Red Sea is usually moderate, a prolonged duration and the existence of a long fetch may give rise to waves that reach up to 3.5 m. The irregular shape of the Red Sea coasts creates shadowing areas, especially in the south where southward moving waves reduce to swell and propagate unidirectionally. During summer, consistent northwesterly winds generate mean wave heights of about 1−1.5 m in the north, frequently exceeding 2 m (Langodan et al. 2014, 2018). The southward wave system persists throughout the year, while the northward system associated with the monsoon winds exhibits a well-defined seasonality between October and April (Langodan et al. 2018). The co-existence of northward and southward waves in winter creates a convergence zone in the central Red Sea (Langodan et al. 2015). Various transversal jets, such as the Tokar jet on the Sudan coast and others that originate in the AP generate locally dominant wave regimes (Langodan et al. 2017b). These exhibit strong seasonality and are usually dominated by other systems.

Ecological indicators through remote sensing: The recent development of multi-sensor based satellite missions, such as the Ocean Colour Climate Change Initiative (OC-CCI), has increased the coverage of surface Chl-a measurements in the Red Sea, by enhancing the retrieval of satellite data under adverse atmospheric conditions (Fig.6). Using recent available in-water measurements of chlorophyll, Brewin *et al.* (2013, 2015, 2019) and Racault *et al.* (2015) have shown that both standard ocean-colour algorithms and the OC-CCI algorithm perform well in the Red Sea, supporting the use of satellite Chl-a datasets and derived ecological indicators.

The open waters of the Red Sea Chl-a depict a distinct seasonality with maximum concentrations seen during wintertime, which we attributed to vertical mixing in the north and wind-induced horizontal intrusion of nutrient-rich water in the south, and minimum concentrations during summer (Raitsos et al. 2013). However, large sporadic blooms have been reported during summer at the coastal Southern Red

Sea (Racault et al. 2015; Dreano et al. 2016). The concentration and the duration of the phytoplankton growing season in the Red Sea are modulated by the strength of the winter monsoon over the Arabian Sea, which affects the horizontal advection of fertile waters from the Indian Ocean (Raitsos et al. 2015). Warmer conditions over the region were also associated with substantially weaker winter phytoplankton blooms, which initiate later and are shorter in their overall duration (~ 4 weeks) (Gittings et al. 2018; Gittings et al. 2019a). Satellite-derived estimates of phytoplankton size structure are in good agreement with the *in situ* measurements, and also capture the spatial variability related to regional mesoscale dynamics (Gittings et al. 2019b). Using high-resolution satellite remote sensing observations, it was further recently shown that satellites successfully detect and generate spatial maps of Harmful Algal Blooms (HABs) associated with different phytoplankton functional types, matching concurrent *in situ* data remarkably well (Gokul et al. 2019).

High-Resolution Nested Modelling in Support of New Mega-Developments along the Red Sea Coast

Met-Ocean modeling in NEOM:

NEOM spreads over an area of 26,500 km^2 along the northern Red Sea coast of Saudi Arabia, bordering Jordan and Egypt. To support environmental impact assessment efforts and to generate essential met-ocean data required for initial planning, high-resolution atmospheric and oceanic models were implemented and nested within the iReds models. A 3-year 600 m resolution WRF simulation was performed to investigate the specific orographic influence on the coastal atmospheric conditions and to drive high-resolution coastal ocean models. Air-quality was also investigated using HYSPLIT driven by the 600 m WRF fields to study dispersion pollutants and their diurnal variations in relation to the land-sea breezes and boundary layer heights (Dasari et al. 2019c).

Our analysis of the large-scale ocean circulation of the NEOM region with MITgcm outputs suggests numerous eddy features with the bathymetry being the critical factor driving their interactions. A coupled Delft3D+SWAN model configuration with horizontal resolution of 50 m and 10 vertical sigma levels was nested within MITgcm to resolve the coastal circulations and forced with tides and 600 m WRF fields. The simulations for different seasons highlighted different coastal circulation features, including a prominent localized eddy-like structure in the center of the NEOM lagoon where the inner water connects with the open ocean through a narrow channel, and a persistent northwest-southeast current along the broad offshore edge of the coral reefs (Fig.7a). The "residence time" estimated based on trajectories of simulated passive particles suggests a faster ventilation rate in winter. The SWAN model nested within the regional WWIII suggested a dominance of locally generated waves in the southeast direction, with a maximum significant wave height of ~0.8 m, associated with consistent strong northwesterlies.

Extreme waves and water levels for King Abdullah Economic City (KAEC): KAEC is a new city under development along the western Saudi coast, comprising the largest port on the Red Sea, residential

districts, and an Industrial Valley. The area is surrounded by coral reefs and includes shallow lagoon on the southern side. We supported the development of the sea wall for coastal protection by providing estimates of extreme wave heights and water levels for the KAEC shoreline. For this, we used a coupled ADCIRC+SWAN model configured on a triangular grid with an open boundary in the Arabian Sea. The model's unstructured grid resolution varied from a maximum vertex spacing of approximately 60 km near the boundary to 60-80 m near the KAEC coastline. A bathymetry was generated 0.5m resolution LiDAR surveys along KAEC coast. Simulations were carried out for a 30-year period, forced with our regional reanalysis. Extreme value analyses were applied to estimate different return levels of wave heights and water levels. The model effectively simulated the dampening of the offshore waves propagating towards the shoreline by the coral reefs (Fig.7b). KAEC coastline being a small tidal regime, the meteorological sea level dominates extreme sea levels, mostly observed during winter. The 100-year return levels of wave heights and water level were estimated at 70 cm and 65 cm, respectively, only marginally (~5 cm) different from the 30-year maxima (Langodan et al. 2019; Antony et al. 2020).

Regional Forecasting Applications

Extreme rainfall forecasting: KSA is characterized by a hot and arid desert climate. Occasionally, extreme precipitation events over the Jeddah region have led to flooding that caused extensive damage in human life and infrastructure (e.g. de Vries et al. 2013). The large-scale features are important factors in producing regional extreme precipitation, which for a particular case, may exceed three times the average annual rainfall. These heavy rainfall events are associated with the northward extension of the Red Sea trough and intensification of the Arabian Anticyclone, which provide warm moist air to the region, creating favorable conditions for the development of a short-lived quasi-stationary mesoscale convective systems (Dasari et al. 2017a). Using a convective-permitting WRF configuration, Viswanadhapalli et al. (2016) assessed the predictability of two extreme rainfall events formed over Jeddah while assimilating various combinations of conventional and satellite observations (Fig.8a). A similar WRF configuration was implemented by Dasari et al. (2017b) to study the Mecca 2016 extreme rainfall event. More recently, Luong et al. (2019) investigated the impact of urbanization using WRF by incorporating an urban canopy model and urban land cover for several extreme weather events over Jeddah and reported that urbanization enhanced rainfall by ~25%.

Oil-spill forecasting: iReds is regularly used to support oil spill prediction efforts. As an example, we have simulated a realistic oil spill scenario to support the Saudi authorities in the southern Red Sea from a deserted oil tanker filled with oil and anchored at Ras-Isa port north of Hudaydah off the coast of Yemen. The ship, which has not been operational since March 2015, is eroding and there are serious concerns that the gas building up in the storage tanks could lead to an explosion that might trigger an oil spill (Meredith 2019). The tanker carries an estimated volume of 1m barrels of crude oil, four times the amount of oil released in the 1989 Exxon Valdez oil spill. MEDSLIK was used to model the transport and fate of oil for

a winter scenario. Forecast winds, waves and ocean currents from iReds during the first two weeks of February 2019 have been used as inputs. The tanker oil was continuously released over a two-week simulation period. Fig.8b shows the concentration of oil (in barrels km^{-2}) after 14 days of spill at the tanker location (15° 15' 11" latitude and 42° 36' 52" longitude). At the end of the simulation period, 20% of the oil evaporated. Following the pattern of the predicted ocean circulation, the oil was transported north-east, where about 60% of its volume washed up onshore. The remaining 20% of the oil formed a surface slick of about 55 km^2 in size.

4. Future Directions

iReds has so far made important contributions in terms of shedding new insights about the regional atmospheric and oceanic circulations, variability and trends of the Red Sea. Outputs from its various long-term simulations established, in particular, a unique basin-wide eddy activity and its driving forces, a prominent seasonally varying overturning circulation modulated by the Indian monsoon, and the occasional fast ventilation of its deep waters through deep water formation events forced by cold weather anomalies in its northern end. The system was further critically important in supporting the undergoing mega-projects along the Red Sea shores, providing unique information about the regional environment to optimize the design and the operations of these new developments. It further provided for the first time regionally-tuned forecasting capabilities that were proven paramount during urgent environmental situations.

We are envisioning, and have already started working along with several directions, to implement new capabilities and continue enhancing iReds performances in the future, while further deepening our understanding of the regional circulation and variability. Our ultimate goal is to develop an integrated data-driven modeling and forecasting system that incorporates all available oceanic and atmospheric observations in the Red Sea region and makes predictions and actionable information available to scientists, government and industry, and non-expert recipients. In this regard, the first operational Red Sea modeling system is expected to be released online in the year 2020, and will subsequently be equipped with state-of-the-art interactive visualization and data analytics.

- *iReds developments*

Beyond the importance of predicting dust and atmospheric pollution, aerosols play a crucial role in the radiation budget and the development of clouds and precipitation. They are also an important source of nutrients for the Red Sea ecosystem. So far, aerosols variations have only been climatologically accounted for in iReds. WRF-Chem is equipped with state-of-the-art modules to simulate and study aerosols, and we have recently implemented it over the AP. We are currently working on developing high-resolution aerosol emission inventories (natural, anthropogenic, and biogenic) on daily-scales by tuning satellite remote sensing retrieval algorithms with available *in situ* measurements. These will be

then incorporated/assimilated into WRF-Chem to simulate and predict dust storms, and outbreaks of industrial and urban haze pollution.

As part of the newly established Center of Excellence for NEOM research at KAUST, our modeling system will be further expanded to investigate oceanic and atmospheric circulations at the urban scales. Work is already undergoing with external collaborators at Imperial College (UK) and Deltares Institute (Netherlands) to build the required Computational Fluid Dynamics (CFD) algorithms in order to downscale our models' outputs and capabilities at these scales. In this regard, we have further recently introduced and successfully tested a new dynamical downscaling algorithm with WRF, based on the Continuous Data Assimilation approach (Desamsetti et al. 2019). Downscaling ensembles from the global operational centers remain computationally demanding, in terms of both computational cost and storage. We will investigate novel approaches for identifying efficient downscaling probabilistic maps through machine and dynamical learning approaches.

In terms of data assimilation, we will continue making use of, and further develop, various aspects of our ensemble system for more efficient incorporation of observations and improved forecasting and reanalysis skills. We are implementing a hybrid variant composed of static and time-evolving members to reduce the computational cost of integrating the ensemble with the models. Proper accounting of model errors, for instance, through stochastic perturbations and forcing ensembles further greatly enhanced the performance of this approach. Developing data-driven approaches for quantifying the uncertainties of such perturbations and eventually estimating their parameters as part of the assimilation process is our next target. To extend the limits of the system predictability, our plans also include the full coupling of WRF- and MITgcm-DART ensembles during forecasting with the physical models and of their respective updates to dynamically exploit the joint observations in both components.

- *General circulation and climate of the Red Sea and their impact on the ecosystem*

While the upper general circulation of the Red Sea is now relatively well-established owing to our recent studies, little is still known about its deep circulation. It has been suggested that a deep overturning cell is present based on chemical tracers, but our ongoing investigations suggest a more complex 3D circulation with the existence of a basin-wide cyclonic gyre in addition to the deep overturning circulation. Understanding the variability and ventilation of the RSDW is needed to advance our understanding of the general circulation of the Red Sea and will be investigated in our future research. We are further implementing very high-resolution (~100m) non-hydrostatic configurations of the MITgcm with unstructured grids to resolve the features in more detail and study the hydraulic control of the water exchange with the Indian ocean through BaM and the water formation and sinking in the north at various temporal scales.

Monitoring the decadal and seasonal variability of Red Sea ecosystem indicators, in relation to the regional environmental conditions and broader climate change, is a necessity for sustainability. We have synergistically combined remotely-sensed ocean color observations with our models' simulations to

investigate various aspects of the Red Sea ecosystem in this historically data-sparse region. Remote sensing will continue to be an integral component of our system, providing information for models' validation and assimilation, and forecasting how the ecosystem indicators would respond to a changing climate. Currently, we are also developing regionally-tuned algorithms for high-resolution satellite sensors (<300m resolution) that would be particularly useful for tackling ecological issues in the coastal economic zone of the Red Sea. In parallel, we will generate interannual simulations with the ecosystem model, which has been only investigated so far with climatological physical forcing. This multidisciplinary approach should offer new insights into the past and current environmental status of the Red Sea coastal zone, identify vulnerable regions, as well as biodiversity hot-spots.

- *Coupled processes, predictability and forecasting at seasonal (S2S) scales and beyond*

The capabilities of the newly developed SKRIPS coupled model are yet to be fully exploited. We will intensify studies with this system to understand the coupled phenomena in the Red Sea region at short- and long-term scales, and how those respond to the global climate dynamics and variations. We are currently examining the outputs of the ocean-waves coupling component to investigate wave-currents interactions and coastal circulations, with particular interest in the water-exchanges near and over the coral reefs. Another proposed development of SKRIPS is the coupling of the atmospheric chemical and marine ecosystem components to investigate regional carbon variations and exchanges.

This coupled system will be at the core of building long-term regional predictive capabilities at the subseasonal-to-seasonal (S2S) through climate scales. We will assess the model predictability of the regional phenomenon at different scales, including extreme weather phenomena (heavy rainfall, air and marine heatwaves). The focus will be on identifying the key factors and dynamical processes that are sources for extended predictability in the region and quantify their impact on the forecasting skills through sensitivity studies. These will be then used as a guide for designing efficient, regionally-tuned, data-driven strategies for projecting the weather and climate of the Red Sea.

Acknowledgments

The development of the Red Sea modeling system is being supported by the Virtual Red Sea Initiative and the Competitive Research Grants (CRG) program from the Office of Sponsored Research at KAUST, Saudi Aramco Company through the Saudi ARAMCO Marine Environmental Center at KAUST, and by funds from KAEC, NEOM and RSP through Beacon Development Company at KAUST. iReds is implemented on the Shaheen-II XC40 – supercomputer at KAUST, a 36-cabinet Cray composed of 6,174 dual socket compute nodes based on 16 core Intel Xeon E5-2698v3 processors running at 2.3GHz. Shaheen has a total of 197,568 processor cores and 790TB of aggregate memory, and is capable of delivering a theoretical peak of 7.2 PFLOP/s.

References

Afzal, S., M. Hittawe, S. Ghani, T. Jamil, O. Knio, M. Hadwiger, and I. Hoteit, 2019a: The state of the art in visual analysis approaches for ocean and atmospheric datasets. Computer Graphics Forum, 38: 881-907.

Afzal, S., S. Ghani, G. Tissington, S. Langodan, H. P. Dasari, D. Raitsos, J. Gittings, T. Jamil, M. Srinivasan, and I. Hoteit, 2019b: RedSeaAtlas: A visual analytics tool for spatio-temporal multivariate data of the Red Sea. Workshop on Visualization in Environmental Sciences (EnvirVis), doi:10.2312/envirvis.20191101.

Albarakati, S., R. M. Lima, L. Giraldi, I. Hoteit, and O. Knio, 2019: Optimal 3D trajectory planning for AUVs using ocean general circulation models. Ocean Engineering, 188, 106266.

Anderson, J., T. Hoar, K. Raeder, H. Liu, N. Collins, R. Torn, and A. Avellano, 2009: The Data Assimilation Research Testbed: A community dacility. Bull. Amer. Meteor. Soc., 90, 1283–1296.

Antony, C., S. Langodan, P. R. Shanas, H. P. Dasari, Y. Abualnaja, O. Knio, and I. Hoteit, 2019: Modelling extreme water levels along the central Red Sea coast of Saudi Arabia-Processes and frequency analysis. Natural Hazards, under review.

Ardhuin, F., E. Rogers, V. Babanin, J. F. Filipot, A. Roland, A. Van der Westhuysen, P. Queffeoulou, J. M. Lefevre, A. Lotfi, and F. Collard, 2010: Semiempirical dissipation source functions for ocean waves. Part I: Definition, calibration and validation. J. Phys. Oceanogr., 40, 1917-1941.

Attada, R., H. P. Dasari, J. S. Chowdary, Y. Ramesh Kumar, O. Knio, and I. Hoteit, 2018a: Surface air temperature variability over the Arabian Peninsula and its links to circulation patterns. Int. J. Climatol., 39(1), 445-464.

Attada R., H. P. Dasari, A. Parekh, J. S. Chowdary, S. Langodan, O. Knio, and I. Hoteit, 2018b: The role of the Indian Summer Monsoon variability on Arabian Peninsula summer climate. Clim. Dyn., 52, 3389, doi: 10.1007/s00382-018-4333-x.

Attada, R., K. Ravi Kumar, Y. Ramesh Kumar, H. P. Dasari, O. Knio, and I. Hoteit, 2018c: Prominent modes of summer surface air temperature variability and associated circulation anomalies over the Arabian Peninsula. Atmos. Sci. Lett., 19:e860, https://doi.org/10.1002/asl.860.

Baretta, J. W., W. Ebenhoh, and P. Ruardij, 1995: The European-Regional-Seas-Ecosystem-Model, a complex marine ecosystem model. Neth. J. Sea Res., 33, 233-246.

Barker, D., X.-Y. Huang, Z. Liu, T. Auligné, X. Zhang, S. Rugg, R. Ajjaji, A. Bourgeois, J. Bray, Y. Chen, M. Demirtas, Y.-R. Guo, T. Henderson, W. Huang, H.-C. Lin, J. Michalakes, S. Rizvi, and X. Zhang, 2012: The Weather Research and Forecasting Model's Community Variational/Ensemble Data Assimilation System: WRFDA. Bull. Amer. Meteor. Soc., 93, 831–843.

Belkin, I. M., 2009: Rapid warming of Large Marine Ecosystems. Prog. Oceanogr., 81, 207–213.

Booij, N., R. C. Ris, and L. H. Holthuijsen, 1999: A third-generation wave model for coastal regions. Part 1: Model description and validation. J. Geophys. Res., 104, 7649-7666.

Bower, A. S., and J. T. Farrar, 2015: Air–Sea Interaction and Horizontal Circulation in the Red Sea. N.M.A. Rasul and I.C.F. Stewart, Eds., Vol. 1900 of Springer Earth System Sciences, Springer Berlin Heidelberg, 329–342.

Brewin B., X. A. G. Morán, D. E. Raitsos, J. Gittings, M. L. Calleja, M. S. Viegas, M. I. Ansari, N. Al-Otaibi, T. M. Huete-Stauffer, and I. Hoteit, 2019: Factors regulating the relationship between

total and size-fractionated chlorophyll-a in coastal waters of the Red Sea. Frontiers in Microbiology, 10, 1964.

Brewin, R. J. W., D. E. Raitsos, G. Dall'Olmo, N. Zarokanellos, T. Jackson, M-F. Racault, E. S. Boss, S. Sathyendranath, B. H. Jones, and I. Hoteit, 2015: Regional ocean-colour chlorophyll algorithms for the Red Sea. Remote Sensing of Environment, 162, 257-270.

Brewin, R. J. W., D. E. Raitsos, Y. Pradhan, and I. Hoteit, 2013: Comparison of chlorophyll in the Red Sea derived from MODIS-Aqua and in vivo fluorescence. Remote Sensing of Environment, 136, 218-224.

Cantin, N. E., A. L. Cohen, K. B. Karnauskas, A. M. Tarrant, and D. C. McCorkle, 2010: Ocean warming slows coral growth in the central Red Sea. Science, 329, 322–325.

Carvalho, S., B. Kürten, G. Krokos, I. Hoteit, and J. Ellis, 2019: The Red Sea. Book Chapter in World Seas: An Environmental Evaluation – vol II: the Indian Ocean to the Pacific, Chapter 3, 49-74.

Cember, R. P. 1988: On the sources, formation, and circulation of Red Sea deep water. J. Geophys. Res., 93, 8175–8191.

Chaidez, V., D. Dreano, S. Agusti, C. M. Duarte, and I. Hoteit, 2017: Decadal trends in Red Sea maximum surface temperature. Sci. Rep., 7, 8144.

Churchill, J. H., Y. Abualnaja, R. Limeburner, and M. Nellayaputhenpeedika, 2018: The dynamics of weather-band sea level variations in the Red Sea. Regional Studies in Marine Science, 24, 336-342.

Collingridge, K., 2012: Modelling risk areas in the North Sea for blooms of the invasive comb jellyfish Mnemiopsis Leidyi. CEFAS Summer Proj., 9, 21–36.

da Silva, J., J. Magalhaes, T. Gerkema, and L. Maas, 2012: Internal solitary waves in the Red Sea: An unfolding mystery. Oceanography, 25, 96–107.

Dasari, H. P., L. Sabique, V. Yesubabu, V. B. Rao, V. P. Papadopoulos, and I. Hoteit, 2017a: ENSO influence on the Red Sea Convergence Zone and Associated Rainfall. Int. J. Climatol., doi:10.1002/joc.5208.

Dasari, H. P., A. Raju, O. Knio, and I. Hoteit, 2017b: Analysis of a severe weather event over Mecca, Kingdom of Saudi Arabia using observations and high-resolution modeling. Meteorological Applications, doi:10.1002/met.1662.

Dasari, H. P., S. Desamsetti, S. Langodan, R. Attada, R. K. Kunchala, Y. Viswanadhapalli, O. Knio, and I. Hoteit, 2019a: High-resolution assessment of solar energy resources over the Arabian Peninsula. Applied Energy, 248, 354-371.

Dasari, H. P., D. Srinivas, S. Langodan, R. Attada, A. Karumuri, and I. Hoteit, 2019b: Multidecadal variability of the Arabian Peninsula rainfall and its relationship with the ENSO signals in the tropical Indo-Pacific. J. Climate, accepted.

Dasari, H. P., S. Desamsetti, S. Langodan, S. Singh, L. N. K. Ramakrishna, and I. Hoteit, 2019c: Air-quality assessment over the World's Most Ambitious Project, NEOM in Kingdom of Saudi Arabia. Atmospheric Environment, under review.

De Dominicis, M., N. Pinardi, G. Zodiatis, and R. Lardner, 2013b: MEDSLIK-II, a Lagrangian marine surface oil spill model for short-term forecasting - Part I: Theory. Geosci. Model. Dev., 6, 1851-1869.

De Dominicis, M., N. Pinardi, G. Zodiatis, and R. Archetti, 2013a: MEDSLIK-II, a Lagrangian marine surface oil spill model for short-term forecasting - Part II: Numerical simulations and validations. Geosci. Model. Dev., 6, 1871-1888.

de Vries, A. J., E. Tyrlis, D. Edry, S. O. Krichak, B. Steil, and J. Lelieveld, 2013: Extreme precipitation events in the Middle East: Dynamics of the Active Red Sea Trough. J. Geophys. Res., 118, 7087-7108.

Deltares, 2016: Delft3D-FLOW. Simulation of multi-dimensional hydrodynamic flow and transport phenomena, including sediments – User Manual, Version 3.15, Deltares, Delft, The Netherlands.

Desamsetti, S., H. P. Dasari, S. Langodan, E. S. Titi, O. Knio, and I. Hoteit, 2019: Efficient dynamical downscaling of general circulation models Using continuous data assimilation. Q. J. Roy. Meteor. Soc., 245, 3175-3194.

Draxler, R. R., and G. D. Hess, 1997: Description of the HYSPLIT_4 modeling system. NOAA Tech. Memo. ERL ARL-224, NOAA/Air Resources Laboratory, Silver Spring, MD, 24 pp.

Dreano, D., D. E. Raitsos, J. Gittings, G. Krokos, and I. Hoteit, 2016: The Gulf of Aden intermediate water intrusion regulates the Southern Red Sea summer phytoplankton blooms. PLoS One, 11(12), e0168440.

Edwards, A., and S. Head, 1986: Red Sea key environment. Headington Hill Hall, Oxford, UK: Pergamon Press.

El Mohtar, S., I. Hoteit, O. Knio, L. Issa, and I. Lakkis, 2018: Lagrangian tracking in stochastic fields with application to an ensemble of velocity fields in the Red Sea. Ocean Modelling, 131, 1-14.

Eshel, G., M. A. Cane, and M. B. Blumenthal, 1994: Modes of subsurface, intermediate, and deep water renewal in the Red Sea. J. Geophys. Res., 99, 15,941-15,952.

Genevier, L. G. C., T. Jamil, D. E. Raitsos, G. Krokos, and I. Hoteit, 2019: Marine heatwaves reveal coral reef zones susceptible to bleaching in the Red Sea. Global Change Biol, 25, 2338-2351.

Gimeno, L., A. Drumond, R. Nieto, R. M. Trigo, and A. Stohl, 2010: On the origin of continental precipitation. Geophys. Res. Let., 37(13), doi:10.1029/2010GL043712.

Gittings, J. A., D. E. Raitsos, G. Krokos, and I. Hoteit, 2018: Impacts of warming on phytoplankton abundance and phenology in a typical tropical marine ecosystem. Sci. Rep., 8, 2240.

Gittings J. A., R. J. W. Brewin, D. E. Raitsos, M. Kheireddine, M. Ouhssain, B. H. Johns, and I. Hoteit, 2019a: Remotely sensing phytoplankton size structure in the Red Sea. Remote Sensing of Environment, 234, 111387.

Gittings, J. A., D. E. Raitsos, M. Kheireddine, M. F. Racault, H. Claustre, and I. Hoteit, 2019b: Evaluating tropical phytoplankton phenology metrics using contemporary tools. Sci. Rep., 9, 674.

Gokul, E. A., D. E. Raitsos, J. A. Gittings, A. Alkawri, and I. Hoteit, 2019: Remotely sensing harmful algal blooms in the Red Sea. PLoS One, 14, doi:10.1371/journal.pone.0215463.

Guo, D. Q., T. R. Akylas, P. Zhan, A. Kartadikaria, and I. Hoteit, 2016: On the generation and evolution of internal solitary waves in the southern Red Sea. J. Geophys. Res., 121, 8566-8584.

Guo, D. Q., A. Kartadikaria, P. Zhan, J. S. Xie, M. J. Li, and I. Hoteit, 2018: Baroclinic tides simulation in the Red Sea: comparison to observations and basic characteristics. J. Geophys. Res., 123, 9389-9404.

Hill, C., C. DeLuca, Balaji, M. Suarez, and A. Silva, 2004: The architecture of the earth system modeling framework. Comp. Sci. Eng., 6, 18–28.

Höllt, T., A. Magdy, G. Chen, G. Gopalakrishnan, I. Hoteit, C. D. Hansen, and M. Hadwiger, 2013: Visual Analysis of Uncertainties in Ocean Forecasts for Planning and Operation of Off-Shore Structures. IEEE Pacific Visualization Symposium, pp. 59-66.

Höllt, T., A. Magdy, P. Zhan, G. Chen, G. Gopalakrishnan, and I. Hoteit, 2014: Ovis: A Framework for Visual Analysis of Ocean Forecast Ensembles. IEEE Transactions on Visualization and Computer Graphics, 20,1114-1126.

Höllt, T., M. Hadwiger, O. Knio, and I. Hoteit, 2015: Probability maps for the visualization of assimilation ensemble flow data. Workshop on Visualization in Environmental Sciences (EnvirVis), pp.43-47.

Hoteit, I., D. T. Pham, M. E. Gharamti and X. Luo, 2015: Mitigating observation perturbation sampling errors in the stochastic EnKF. Mon. Wea. Rev., 143, 2918-2936.

Ioc, I., 2003: BODC 2003 - Centenary Edition of the GEBCO Digital Atlas, published on CD-ROM on behalf of the Intergovernmental Oceanographic Commission and the International Hydrographic Organization as part of the General Bathymetric Chart of the Oceans, British oceanographic data centre, Liverpool.

Krokos, G., V. P. Papadopoulos, S. S. Sofianos, H. Ombao, P. Dybczak, and I. Hoteit, 2019a: Natural climate oscillations may counteract Red Sea warming over the coming decades. Geophys. Res. Lett., 46, 3454-3461.

Krokos, G., I. Cerovečki, P. Zhan, M. C. Hendershott and I. Hoteit, 2019b: Seasonal evolution of the Mixed layers in the Red Sea. J. Geophys. Res., under review.

Kunchala, R., R. Attada, H. P. Dasari, V. R. Kumar, S. Langodan, Y. Abualnaja, and I. Hoteit, 2018: Aerosol optical depth variability over the Arabian Peninsula using satellite and ground based observations. Atmospheric Environment, 187, 346-357.

Kunchala, R. K., R. Attada, H. P. Dasari, K. Ramesh, Y. Abualnaja, K. Ashok, and I. Hoteit, 2019: On the recent amplification of dust over the Arabian Peninsula during 2002-2012. J. Geophys. Res., doi: 10.1029/2019JD030695.

Langodan, S., L. Cavaleri, Y. Viswanadhapalli, and I. Hoteit, 2014: The Red Sea: a natural laboratory for wind and wave modeling. J. Phys. Oceanogr. 44, 3139-3159.

Langodan, S., L. Cavaleri, Y. Viswanadhapalli, and I. Hoteit, 2015: Wind-wave source functions in opposing seas. J. Geoph. Res., 120, 6751-6768.

Langodan, S., Y. Viswanadhapalli, H. P. Dasari, O. Knio, and I. Hoteit, 2016a: A high resolution assessment of wind and wave energy potentials in the Red Sea. Applied Energy, 181, 244-255.

Langodan, S., V. Yesubabu, and I. Hoteit, 2016b: Impact of atmospheric data assimilation on waves in the Red Sea. Ocean Engineering, 116, 200-215.

Langodan, S., L. Cavaleri, A. Pomaro, V. Yesubabu, L. Bertotti, and I. Hoteit, 2017a: The climatology of the Red Sea – Part 1: The winds. Int. J. Climatol., 37, 4518-4528.

Langodan, S., L. Cavaleri, A. Pomaro, V. Yesubabu, L. Bertotti, and I. Hoteit, 2017b: The climatology of the Red Sea – Part 2: The waves. Int. J. Climatol., 37, 4518-4528.

Langodan, S., L. Cavaleri, Y. Vishwanadhapalli, A. Pomaro, L. Bertotti, and I. Hoteit, 2017a: The climatology of the Red Sea–part 1: the wind. Int. J. Climatol., 37, 4509-4517.

Langodan, S., L. Cavaleri, A. Pomaro, J. Portilla, Y. Abualnaja, and I. Hoteit, 2018: Unraveling climatic wind and wave trends in the Red Sea using wave spectra partitioning. J. Climate, 31, 1881-1895.

Langodan, S., L. Cavaleri, J. Portilla, Y. Abualnaja, and I. Hoteit, 2019: Can we extrapolate climate in an inner basin? The case of the Red Sea. Global and Planetary Change, under review.

Langodan, S., C. Antony, P.R. Shanas, H. P. Dasari, Y. Abualnaja, O. Knio, and I. Hoteit, 2019b: Wave modeling of a reef-sheltered coastal zone in the Red Sea. Ocean Engineering, under review.

Luettich, R.A., and J. J. Westerink, 2004: Formulation and numerical implementation of the 2D/3D ADCIRC finite element model Version 44.XX. ADCIRC Tech. Rep., 74 pp.

Luong, T. M., H. P. Dasari, and I. Hoteit, 2019: Impact of urbanization on the simulation of extreme rainfall in Jeddah, Saudi Arabia. Journal of Applied Meteorology and Climatology, under review.

Marshall, J., A. Adcroft, C. Hill, L. Perelman, and C. Heisey, 1997a: A finite-volume, incompressible Navier Stokes model for studies of the ocean on parallel computers. J. Geophys. Res., 102, 5753-5766.

Marshall, J., C. Hill, L. Perelman, and A. Adcroft, 1997b: Hydrostatic, quasi-hydrostatic, and nonhydrostatic ocean modeling. J. Geophys. Res., 102, 5733-5752.

Meredith, S., 2019: 'Floating bomb': Decaying oil tanker near Yemen coast could soon explode, experts warn. CNBC, 24 July 2019, https://www.cnbc.com/2019/07/24/oil-tanker-near-yemen-coast-could-soon-explode-experts-warn.html, accessed on 12 December 2019.

Nanninga, G. B., P. Saenz-Agudelo, P. Zhan, I. Hoteit, and M. L. Berumen, 2015: Not finding Nemo: limited reef-scale retention in a coral reef fish. Coral Reefs, 34, 383-392.

Osman, E. O., D. J. Smith, M. Ziegler, B. Kürten, C. Conrad, K. M. El-Haddad, C.R. Voolstra, and D. J. Suggett, 2018: Thermal refugia against coral bleaching throughout the northern Red Sea. Global Change Biology, 24, 474–484.

Papadopoulos, V. P., Y. Abualnaja, S. A. Josey, A. S. Bower, D. E. Raitsos, H. Kontoyiannis, and I. Hoteit, 2013: Atmospheric Forcing of the Winter Air–Sea Heat Fluxes over the Northern Red Sea. J. Clim., 26, 1685–1701.

Paris, C. B., J. Helgers, E. van Sebille, and A. Srinivasan, 2013: Connectivity Modeling System: A probabilistic modeling tool for the multi-scale tracking of biotic and abiotic variability in the ocean. Environ. Modell. Softw., 42, 47-54.

Petihakis, G., G. Triantafyllou, I. J. Allen, I. Hoteit, and C. Dounas, 2002: Modelling the spatial and temporal variability of the Cretan Sea ecosystem. J. Mar. Sys., 36, 173-196.

Raboudi, N. F., B. Ait-El-Fquih, and I. Hoteit, 2018: Ensemble Kalman filtering with one-step-ahead smoothing. Mon. Wea. Rev., 146, 561-581.

Racault, M.-F., D. E. Raitsos, M. L. Berumen, R. J. W. Brewin, T. Platt, S. Sathyendranath, and I. Hoteit, 2015: Phytoplankton phenology indices in coral reef ecosystems: Application to ocean-color observations in the Red Sea. Remote Sensing of Environment, 160, 222-234.

Raitsos, D. E., I. Hoteit, P. K. Prihartato, T. Chronis, G. Triantafyllou, and Y. Abualnaja, 2011: Abrupt warming of the Red Sea. Geophys. Res. Lett., 38, doi:10.1029/2011GL047984.

Raitsos, D. E., Y. Pradhan, R. J. W. Brewin, G. Stenchikov, and I. Hoteit, 2013: Remote sensing the phytoplankton seasonal succession of the Red Sea. PLoS One, 8, e64909,

doi:10.1371/journal.pone.0064909.

Raitsos, D. E., X. Yi, T. Platt, M.-F. Racault, R.J.W. Brewin, Y. Pradhan, V.P. Papadopoulos, S. Sathyendranath, and I. Hoteit, 2015: Monsoon oscillations regulate fertility of the Red Sea. Geophys. Res. Lett., 42, 855-862.

Raitsos, D. E., R. J. W. Brewin, P. Zhan, D. Dreano, Y. Pradhan, G. B. Nanninga, and I. Hoteit, 2017: Sensing coral reef connectivity pathways from space. Sci. Rep., 7, 9338.

Ralston, D. K., H. Jiang, and T. F. Ferrar, 2013: Waves in Red Sea: Response to monsoonal and mountain gap winds. Continental Shelf Research, 65, 1-13.

Sivareddy, S., H. Toye, P. Zhan, S. Langodan, G. Krokos, O. Knio, and I. Hoteit, 2019: Impact of Atmospheric and Model Physics Perturbations on a High-Resolution Ensemble Data Assimilation System of the Red Sea. Journal of Geophysical research, under review.

Skamarock, W.C., and Coauthors, 2008: A description of the Advanced Research WRF version 3. NCAR Tech Note NCAR/TN-475+STR, 125 pp.

Sofianos, S., and W. E. Johns, 2007: Observations of the summer Red Sea circulation. J. Geophys. Res., 112, 1–20.

Sofianos, S., and W. E. Johns, 2015: The Red Sea: Water mass formation, Overturning Circulation, and the Exchange of the Red Sea with the Adjacent Basins. (N. M. A. Rasul & I. C. F. Stewart, Eds.). Berlin, Heidelberg: Springer Berlin Heidelberg.

Stammer, D., C. Wunsch, R. Giering, C. Eckert, P. Heimbach, J. Marotzke, A. Adcroft, C. N. Hill, and J. Marshall, 2002: The global ocean circulation during 1992–1997, estimated from ocean observations and a general circulation model. J. Geophys. Res., 107, 3118.

Sun, R., A. C. Subramanian, A. J. Miller, M. R. Mazloff, I. Hoteit, and B. D. Cornuelle, 2019: SKRIPS v1. 0: a regional coupled ocean-atmosphere modeling framework (MITgcm-WRF) using ESMF/NUOPC, description and preliminary results for the Red Sea. Geosci. Model. Dev., 12, 4221–4244.

Tolman, H. L., 2008: User manual and system documentation of WAVEWATCH-III version 3.14. Technical Note Nr.268, pp.25-32, NOAA/NWS/NCEP/OMB.

Toye, H., P. Zhan, G. Gopalakrishnan, A. R. Kartadikaria, H. Huang, O. Knio, and I. Hoteit, 2017: Ensemble data assimilation in the Red Sea: sensitivity to ensemble selection and atmospheric forcing. Ocean Dynamics, 67, 915-933.

Toye, H., S. Kortas, P. Zhan, and I. Hoteit, 2018: A fault-tolerant HPC scheduler extension for large and operational ensemble data assimilation: Application to the Red Sea. J. Comp. Sci., 27, 46-56.

Toye, H., S. Sivareddy, N. Raboudi, and I. Hoteit, 2019: A Hybrid ensemble data assimilation system for the Red Sea: Implementation and Evaluation. Q. J. R. Meteo. Soc., under review.

Triantafyllou, G., F. Yao, G. Petihakis, K. Tsiaras, D. E. Raitsos, and I. Hoteit, 2014: Exploring the Red Sea seasonal ecosystem functioning using a three-dimensional biophysical model. J. Geophys. Res., 119, 1791-1811.

Viswanadhapalli, Y., C. V. Srinivas, S. Langodan, and I. Hoteit, 2016: Predicting extreme rainfall events over Jeddah, Saudi Arabia: impact of data assimilation with conventional and satellite observations. Q. J. Roy. Meteor. Soc., 142, 327-348.

Viswanadhapalli, Y., H. P. Dasari, S. Langodan, V. S. Challa, and I. Hoteit, 2017: Climatic features of the Red Sea from a regional assimilative model. Int. J. Climatol., 37, 2563–2581.

Viswanadhapalli, Y., H. P. Dasari, S. Dwivedi, V. R. Madineni, S. Langodan, and I. Hoteit, 2019: Variability of monsoon low-level jet and associated rainfall over India. Int. J. Climatol., doi:10.1002/joc.6256.

Wang, T., Le Maître, I. Hoteit, and O. Knio, 2016: Path planning in uncertain flow fields using ensemble method. Ocean Dynamics, 66, 1231-1251.

Wang, Y., D. E. Raitsos, G. Krokos, J. A. Gittings, P. Zhan, and I. Hoteit, 2019: Physical connectivity simulations reveal dynamic linkages between coral reefs in the southern Red Sea and the Indian Ocean. Sci. Rep., 9, 16598.

Xie, J. S., G. Krokos, S. Sofianos, and I. Hoteit, 2019: Interannual Variability of the Exchange Flow Through the Strait of Bab-al-Mandeb. J. Geophys. Res., 124, 1988-2009.

Yao, F. C., I. Hoteit, L. J. Pratt, A. S. Bower, A. Kohl, G. Gopalakrishnan, and D. Rivas, 2014a: Seasonal overturning circulation in the Red Sea. Part-II: Winter circulation. J. Geophys. Res., 119, 2263-2289.

Yao, F. C., I. Hoteit, L. J. Pratt, A. S. Bower, P. Zhai, A. Kohl, and G. Gopalakrishnan, 2014b: Seasonal overturning circulation in the Red Sea. Part-I: Model validation and summer circulation. J. Geophys. Res., 119, 2238-2262.

Yao, F., and I. Hoteit, 2018: Rapid red sea deep water renewals caused by volcanic eruptions and the north Atlantic oscillation. Science advances, 4(6), eaar5637.

Zhan, P., A. C. Subramanian, F. C. Yao, and I. Hoteit, 2014: Eddies in the Red Sea: A statistical and dynamical study. J. Geophys. Res., 119, 3909-3925.

Zhan, P., F. C. Yao, A. R. Kartadikaria, Y. Viswanadhapalli, G. Gopalakrishnan, and I. Hoteit, 2015: Far-Field ocean conditions and concentrate discharges modeling along the Saudi coast of the Red Sea. Environ. Sci. Eng., 501-520, doi:10.1007/978-3-319-13203-7-21.

Zhan, P., A. C. Subramanian, F. C. Yao, A. R. Kartadikaria, D. Q. Guo, and I. Hoteit, 2016: The eddy kinetic energy budget in the Red Sea. J. Geophys. Res., 121, 4732-4747.

Zhan, P., G. Gopalakrishnan, A. C. Subramanian, D. Guo, and I. Hoteit, 2018: Sensitivity Studies of the Red Sea Eddies Using Adjoint Method. J. Geophys. Res., 123, 8329-8345.

Zhan, P., G. Krokos, D. Q. Guo, and I. Hoteit, 2019: Three-Dimensional Signature of the Red Sea Eddies and Eddy-Induced Transport. Geophys. Res. Lett., 46, 2167-2177.

Supplementary Materials

Datasets and observations: We make use of a variety of available in situ and satellite observations, and various reanalysis datasets to study the regional ocean and atmospheric variabilities and changes, to validate our models, for prescribing model boundary conditions, and for initialization and assimilation. We have also developed regionally-tuned remote sensing algorithms, based on local observations, to generate improved Chlorophyll datasets for the Red Sea region (Brewin et al., 2019). Details of the datasets, and their use, are listed in Table below.

Datasets	**Type**	**Usage**
Atmospheric Datasets		
ERA-Interim, NCEP FNL, Real-time Global SST, CCMP, CRU	Reanalyses	Initialization and Boundaries
AMSU, QuikSCAT, ASCAT, GPSRO	Satellite	
TRMM, CMORPH, APHRODITE	Rainfall reanalysis	Model validation
Rain gauge precipitation, AWS-PME, KSA Saudi Aramco, KSA RADAR, PME, KSA KAUST-WHOI BUOY Synoptic and Upper - Uni. of Wyoming	Local Met-Ocean	Assimilation and validation
Globwave altimeter wave data	Significant wave height	Wave model validation
Oceanic Datasets		
ECCO2, WOA, GLORYS2	Reanalyses	Initialization and Boundaries
AVHRR, RADS	Satellite	Assimilation and validation
RSP, NEOM, Saudi Aramco Tidal Gauges, KAUST-WHOI BUOY	In-situ Observations	Model validation
OSTIA, AVISO	Satellite	
OTIS	Simulation	Tidal forcing
ESA: Ocean Colour Climate Change Initiative – OC-CCI and Sentinel-3 OLCI	Satellite	Ocean colour / Ecological Indicators

Figures

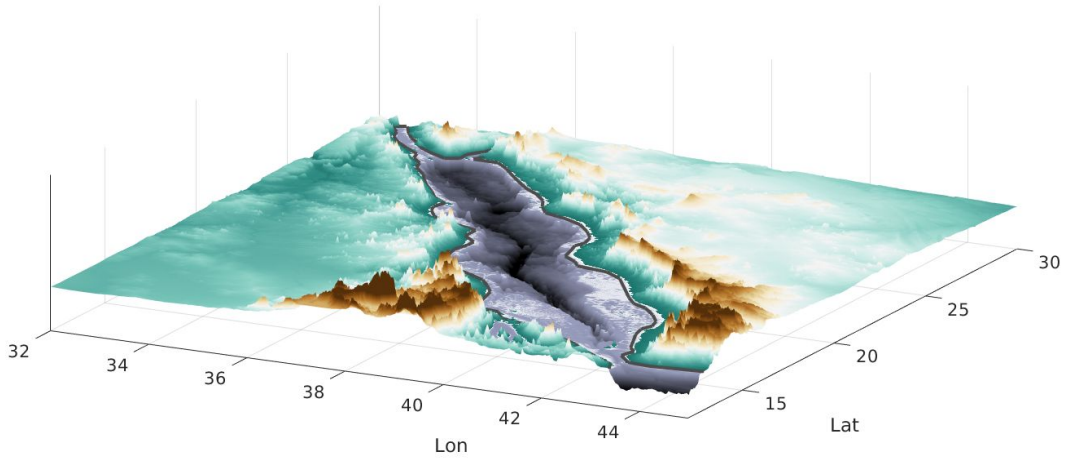

Figure 1. Topography of the Red Sea region.

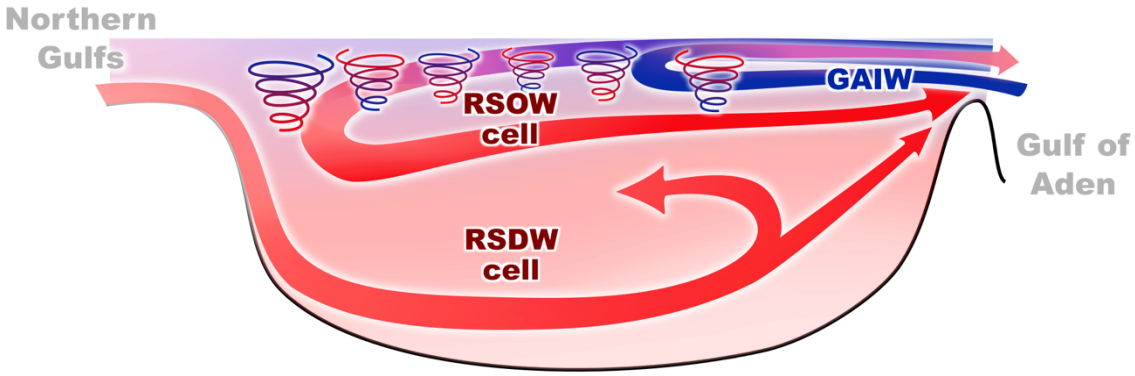

Figure 2. Schematic representation of the main thermohaline cells in the Red Sea circulation (adapted from Sheppard C. (Ed.), 2018). Blue colors represent fresher waters while red colors saline and denser water masses. Mesoscale features, cyclonic and anti-cyclonic eddies, are represented by spirals.

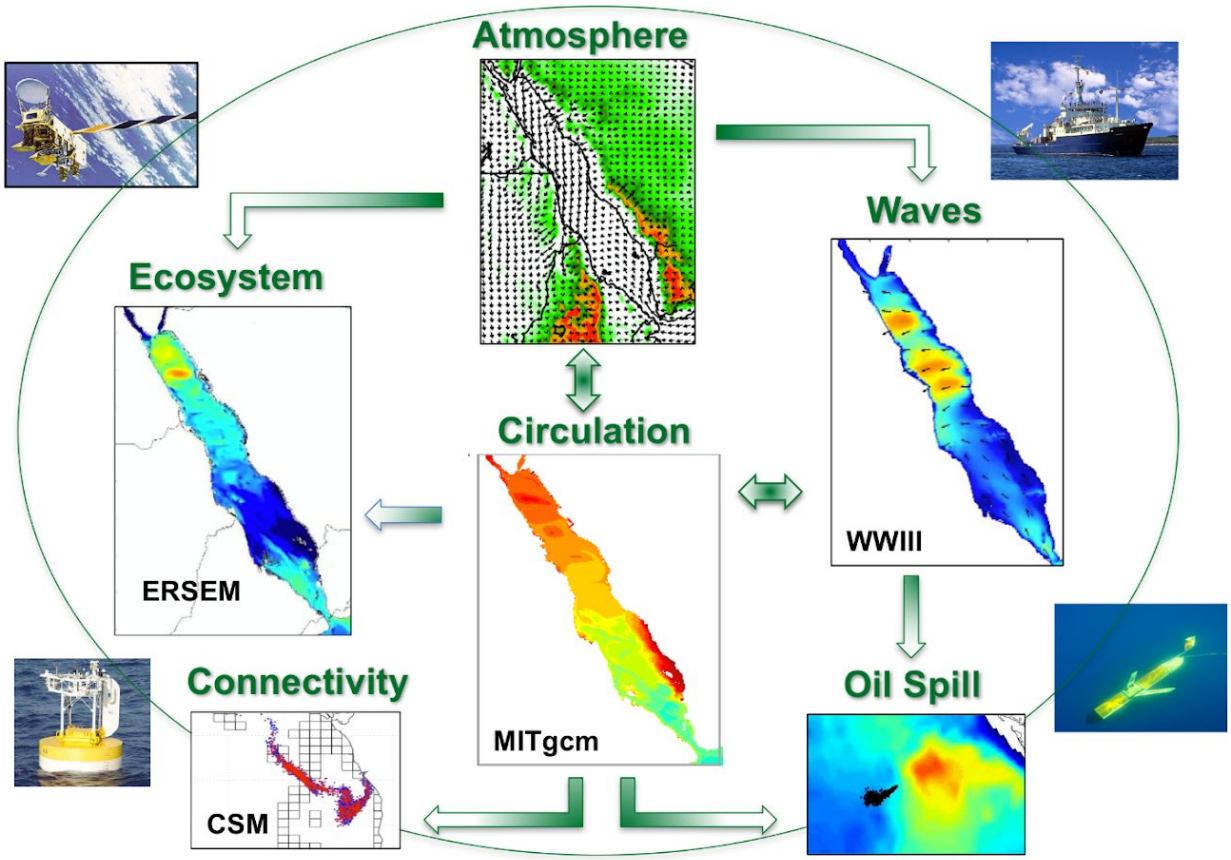

Figure 3. Schematic illustration of the data-driven Red Sea modelling and prediction system.

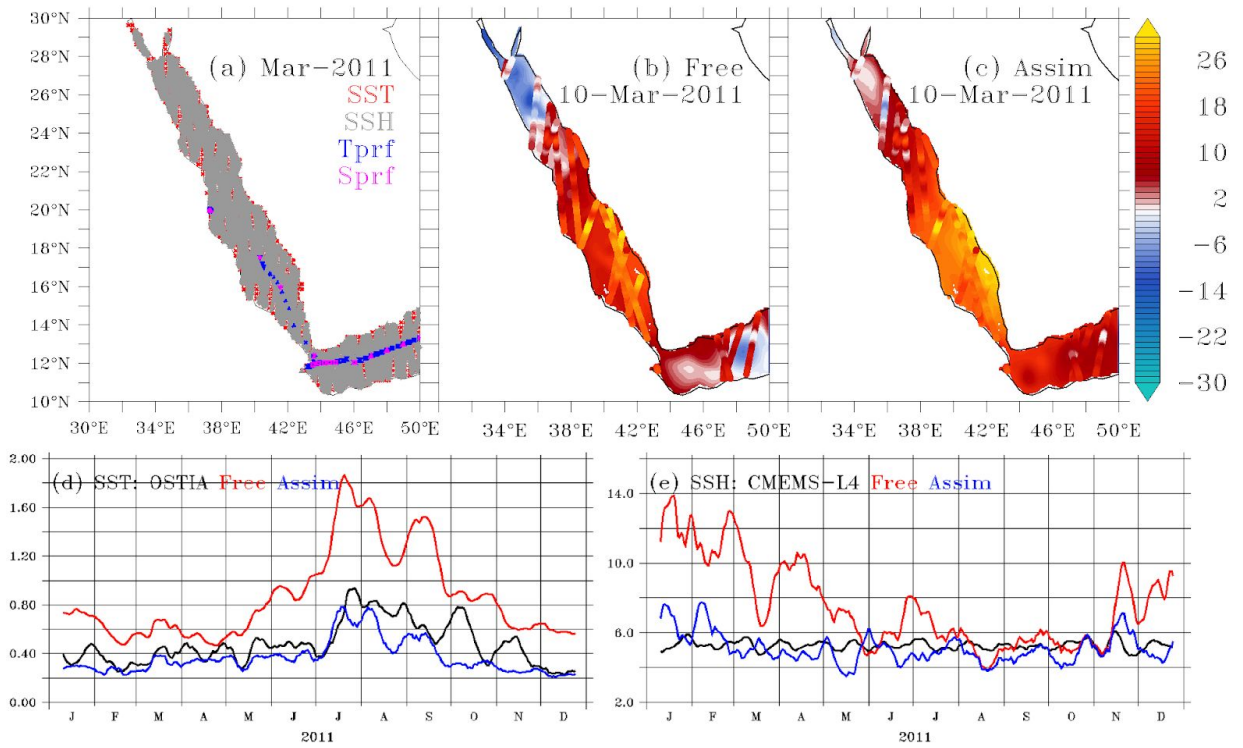

Figure 4. Impact of assimilation in the ocean data assimilation system, DART-MITgcm. Panel (a) display the spatial distribution of SST, SSH, and in-situ temperature and salinity observations that were assimilated in the DART-MITgcm ocean ensemble system during an arbitrary month (March 2011). Panels (b) and (c) respectively show 3-day averaged SSH as resulted from free-model and assimilation runs on an arbitrary day (10th March, 2011). Along-track altimeter SSH observations (between 9-11 March, 2011) are overlaid on these maps to showcase the positive impact of assimilation. Panels (d) and (e) display time series of forecast Root-Mean-Square-Error (RMSE) for SST (°C) and SSH (cm), respectively. Black, red and blue curves correspond to RMSEs in interpolated level-4 gridded product OSTIA for SST and CMEMS-L4 for SSH (daily available on 5km and 25km grids, respectively), and free-model and assimilative-model runs, respectively. On average, assimilation reduces the forecast RMSEs by 1°C for SST and 8cm for SSH. It can further be noted that both SST and SSH observations are better represented in the assimilated solution, even compared to the corresponding interpolated level-4 products, suggesting efficient assimilation of sparse-observations by our DART-MITgcm system.

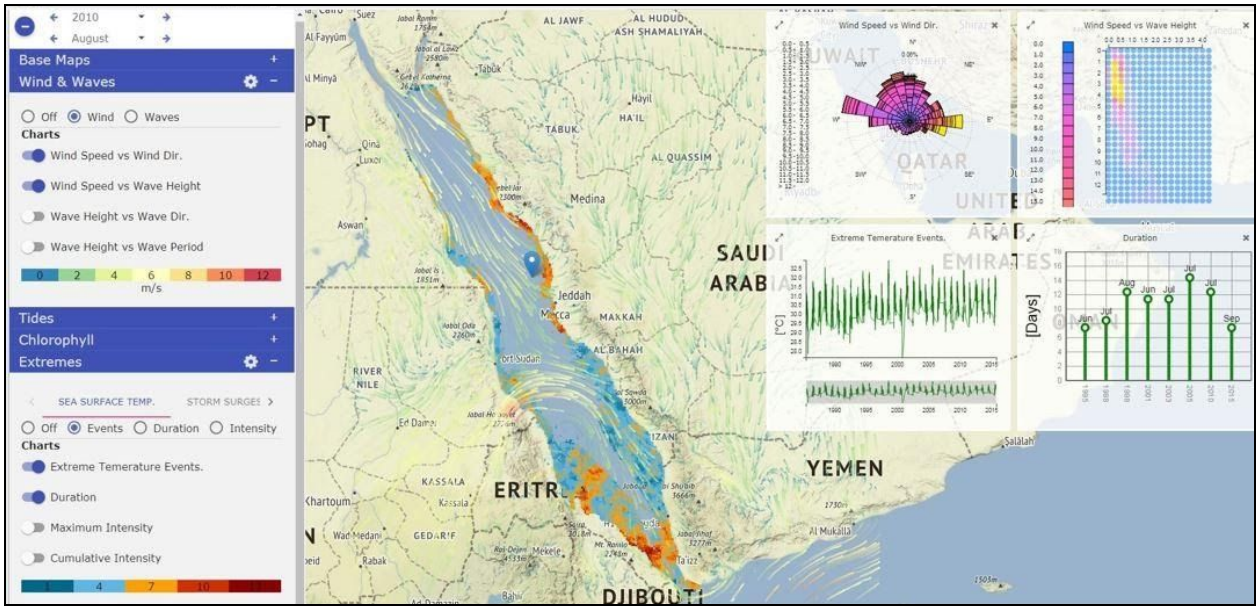

Figure 5. The 'RedSeaAtlas' system showing overall wind patterns and statistics of extreme temperature events in the Red Sea. Users can select any region to show more detailed information and associated attributes through different charts (Afzal et al., 2019).

Figure 6. Remotely-sensed ocean colour observations portraying surface flow (eddies and currents) between coral reefs in the Red Sea. (a-d), Chlorophyll (mg/m3) patterns during different time periods (1-Jun-2010, 21-Jun-2009, 4-Mar-2006, and 13-Apr-2001, respectively). The central map depicts sea-floor elevation and the position of coral reefs (red circles) in the Red Sea (coral reef positions were acquired from: Global Distribution of Coral Reefs, 2010). (e) Simulated particle dispersion trajectories forming pathways of connectivity in the Red Sea. Particles were released from the locations of the coral reefs along the east coast of the central Red Sea. The different colours denote each of the five different Red Sea provinces (Raitsos et al., 2013). The panel suggests basin-wide connectivity with the central Red Sea, except for the southern Red Sea which connects more with the Gulf of Aden (Raitsos et al., 2017; Wang et al., 2019).

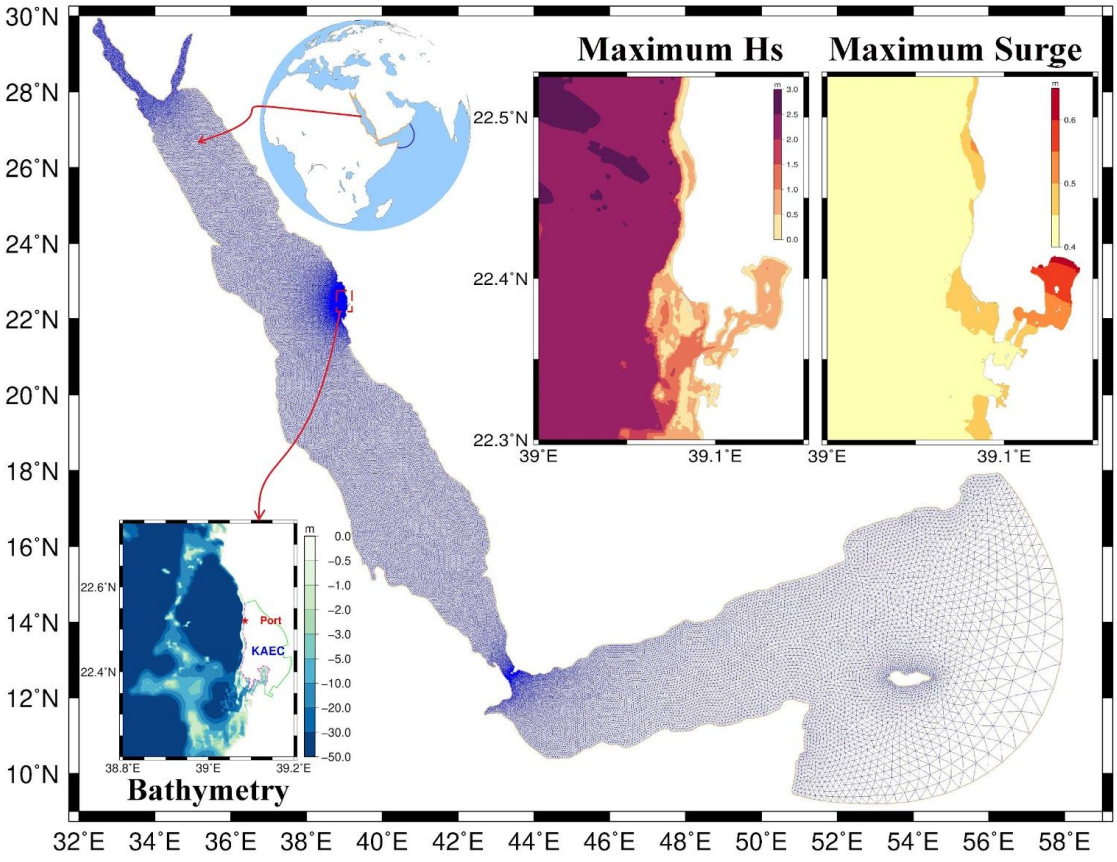

Figure 7. Coupled ADCIRC+SWAN model domain used for estimating extreme wave heights and water levels along the KAEC coastline. The unstructured grid resolution varies from 60 km near the boundary in the Arabian Sea to 60-80 m near the KAEC coastline. The bathymetry of the KEAC and maximum of significant wave heights and water levels from 30-year simulations are also shown in inset images.

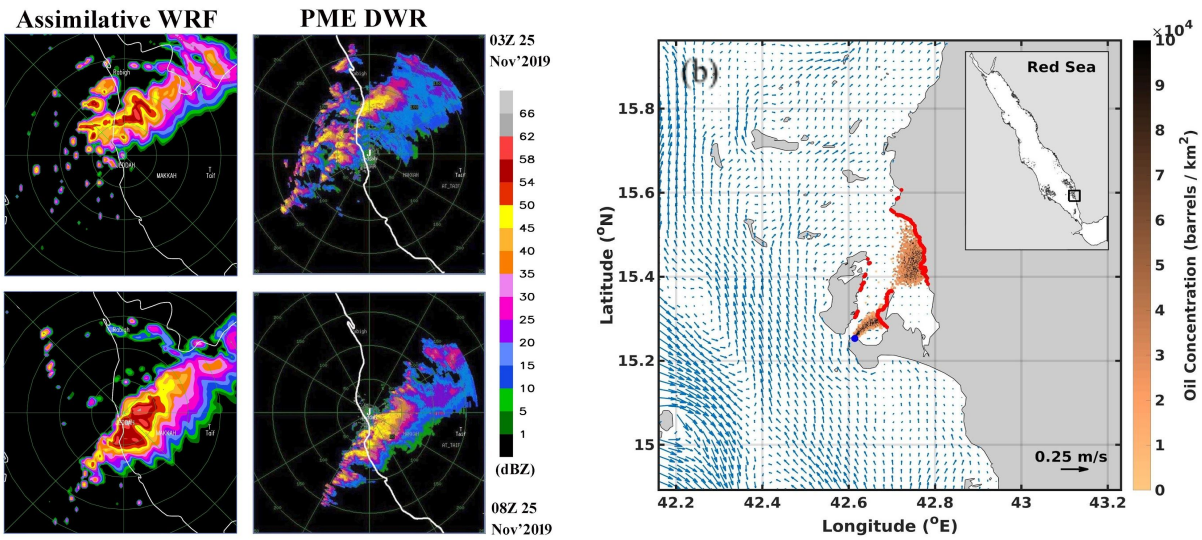

Figure 8. (a) Evolution of reflectivity as forecasted by WRF with assimilation of conventional and satellite radiance data against PME DWR data during Jeddah extreme rainfall event at 0300 UTC, and 0800 UTC on 25 November 2009. (b) Concentration of oil (in barrels/km2) after 14 days of spill from the tanker location marked by the blue dot.